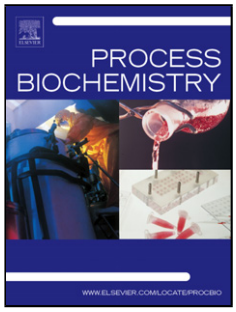

Title: Induction of resveratrol biosynthesis in *Vitis amurensis* cells by heterologous expression of the *Arabidopsis* constitutively active, Ca^{2+}-independent form of the *AtCPK1* gene

Author: <ce:author id="aut0005" author-id="S1359511316309564-a325d4edcb6033b1daa90dd3170295ca"> G.N. Veremeichik<ce:author id="aut0010" author-id="S1359511316309564-4c3bf65af93783b00d5ebf923cd07a41"> V.P. Grigorchuk<ce:author id="aut0015" author-id="S1359511316309564-7afb35255dfed6a1c929afef3571c577"> Y.N. Shkryl<ce:author id="aut0020" author-id="S1359511316309564-97df09882272c42a68926fb7e78a03fc"> D.V. Bulgakov<ce:author id="aut0025" author-id="S1359511316309564-911e9378b86567be70e91a6bfa0164f1"> S.A. Silantieva<ce:author id="aut0030" author-id="S1359511316309564-e47b89bb4efd681e56b6e68f772870cb"> V.P. Bulgakov

PII: S1359-5113(16)30956-4
DOI: http://dx.doi.org/doi:10.1016/j.procbio.2016.12.026
Reference: PRBI 10898

To appear in: *Process Biochemistry*

Received date: 27-11-2016
Accepted date: 30-12-2016

Please cite this article as: Veremeichik GN, Grigorchuk VP, Shkryl YN, Bulgakov DV, Silantieva SA, Bulgakov V.P.Induction of resveratrol biosynthesis in Vitis amurensis cells by heterologous expression of the Arabidopsis constitutively active, Ca2+-independent form of the AtCPK1 gene.*Process Biochemistry* http://dx.doi.org/10.1016/j.procbio.2016.12.026

Induction of resveratrol biosynthesis in *Vitis amurensis* cells by heterologous expression of the *Arabidopsis* constitutively active, Ca^{2+}-independent form of the *AtCPK1* gene

Running Title: CDPK effect on resveratrol production

G.N. Veremeichik[1], V.P. Grigorchuk[1, 2], Y.N. Shkryl[1, 3] *, D.V. Bulgakov[1], S.A. Silantieva[1], V.P. Bulgakov[1, 3]

[1] Institute of Biology and Soil Science of the Far East Branch of the Russian Academy of Sciences, Vladivostok 690022, Russia

[2] Institute of Marine Biology of the Far East Branch of the Russian Academy of Sciences, Vladivostok 690041, Russia

[3] Far Eastern Federal University, Vladivostok 690950, Russia

*Corresponding author

Address: Yury N. Shkryl, Institute of Biology and Soil Science,

159 Stoletija Str., Vladivostok, 690022, Russia

Fax: +7-4232-310193

E-mail: yn80@mail.ru

Graphical abstract

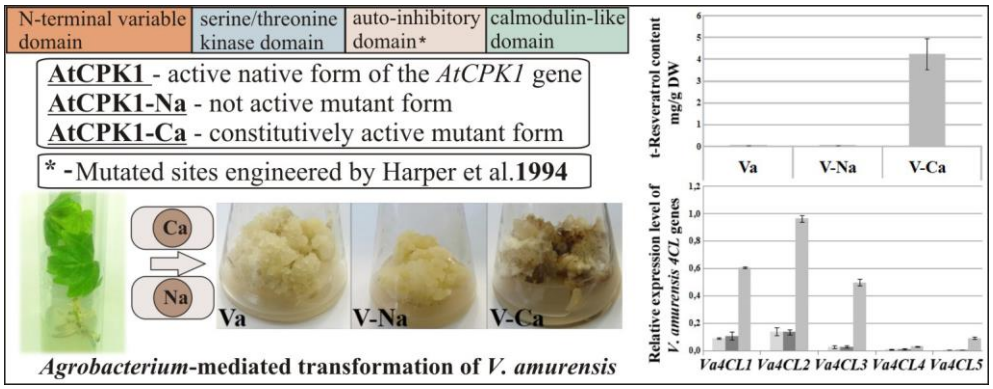

HIGHLIGHTS

- Mutant isoforms of the *AtCPK1* gene were overexpressed in *V. amurensis* calli.
- Constitutively active isoform of the *AtCPK1* gene stimulates resveratrol biosynthesis.
- Effect of *AtCPK1* is an indirect process and is a part of general defense reactions.
- The work may be helpful in metabolic engineering of plant secondary products.

ABSTRACT

In the present study, we established transgenic calli of *Vitis amurensis* that expressed a constitutively active, Ca^{2+}-independent form of the *AtCPK1* gene (*AtCPK1-Ca*) and calli with a non-active form of the gene. High-performance liquid chromatography with UV and high-resolution mass-spectrometry revealed that the predominant metabolites synthesized in our transgenic callus cultures were *trans*-resveratrol di-glucoside, *trans*-piceid, *trans*-resveratrol, *trans*-ε-viniferin and *trans*-δ-viniferin. The resveratrol content in the *AtCPK1-Ca*-transformed callus cultures exceeded that in the control cultures up to 90-fold. Furthermore, the expression of the *AtCPK1-Ca* gene caused cell growth activation, which led to the enhancement of resveratrol production up to 137 times that of the control calli (69.7 mg L^{-1} *vs*. 0.51 mg L^{-1}). Real-time PCR analysis showed that *AtCPK1-Ca* overexpression caused increasing of the expression of the key enzymes of phenylpropanoid pathway of resveratrol biosynthesis, 4-coumarate-CoA ligases. Thus, heterologous expression of constitutively active *CDPK* genes can be used to bioengineer plant cell cultures that produce stilbenes. Possible mechanisms for AtCPK1-mediated signal transduction were proposed by the reconstruction of known protein-protein interactions within CPK1-assotiated protein modules.

KEYWORDS: calcium-dependent protein kinase; *Vitis amurensis*; resveratrol; 4-coumarate-CoA ligases; callus culture; metabolic engineering

Introduction

Resveratrol (3,5,4-trihydroxystilbene) is a secondary metabolite that accumulates in plants in response to microorganism attack [1]. Resveratrol is widely known as a valuable natural stilbene used for a wide range of biomedical applications [2]. However, extraction of resveratrol from wild-growing or cultivated plants often suffers from low abundance of this compound in natural material [3] while complexity of synthetic pathway constrain the industrial application of chemical synthesis [4]. Thus, biotechnological methods utilizing microbial systems and plant cell cultures are the most promising ways for large-scale resveratrol production [5, 6].

Resveratrol is produced from *p*-coumaric acid, which is converted by the action of 4-coumarate-CoA ligase (4CL) into coumaroyl-CoA. Then coumaroyl-CoA and three units of malonyl-CoA are condensed into resveratrol by the action of stilbene synthase (STS) [7]. Heterologous expression of 4CL and STS genes in *Escherichia coli* and *Saccharomyces cerevisiae* grown in the presence of 4-coumaric acid was sufficient for resveratrol synthesis in the recombinant strains [5]. Yet, plasmid instability and cell physiology severely decreased process productivity [8] For that reason, increasing resveratrol production in stable transgenic plant cell cultures is a promising goal for plant biotechnologists. However, overexpression of key genes involved in the synthesis of resveratrol in plant cells did not increase significantly its production levels [9]. The use of regulatory genes for the improvement of resveratrol production could be taken into consideration for further analysis.

It is known that Ca^{2+} and its sensors, calmodulins and calcium-dependent protein kinases, play important roles in the regulation of secondary metabolism [10]. To the best of our knowledge, calmodulin genes have not been used to engineer plant secondary metabolic processes; however, a few reports examining *Arabidopsis CPK1* (calcium-dependent protein kinase 1) indicate that CDPKs may have a promising role in engineering such processes [11, 12]. Calcium-dependent protein kinases are molecular switches and signal responders that regulate plant growth and development, as well as abiotic and biotic stress responses [13]. CDPKs can sense Ca^{2+} and convert developmental and environmental signals into phosphorylation events.

CDPK proteins comprise four functional domains: an N-terminal variable domain, a serine/threonine kinase domain, an auto-inhibitory domain (AID) and a regulatory calmodulin-like domain (CaM-LD). The AID contains a pseudo-substrate sequence that can interact with the active site and inhibit kinase activity [14, 15].

AtCPK1 (http://www.uniprot.org/uniprot/Q06850) acts as a positive regulator to control stress signal transduction in plants [16, 17, 18], controls SA accumulation and pathogen resistance in *Arabidopsis* [19]. Expression of the native *AtCPK1* gene in tomato protoplasts activates NADPH oxidases and leads to an oxidative burst [20]. Harper and colleagues [16] generated a mutant constitutively active gene via deletion of the AID domain. The AID functions as an autoinhibitor, and a six-residue substitution in this domain leads to production of Ca^{2+}-independent enzyme mutant form, with 86% the activity of the native form [16]. In the present study, we used this constitutively active gene (termed *AtCPK1-Ca* in this work). Previous investigation showed the high activity of *AtCPK1-Ca* in stimulating the biosynthesis of anthraquinones [11]. The aim of the present work was to investigate the effects of constitutively active *AtCPK1-Ca* on resveratrol production.

Materials and methods

Callus cultivation

An untransformed callus line of *Vitis amurensis* Rup (*Vitaceae*) (designated as Va in this work) served as a control and was cultivated in 100 mL Erlenmeyer flasks on $W_{B/A}$ medium supplemented with 6-benzylaminopurine (0.5 mg L^{-1}) and α-naphthaleneacetic (2.0 mg L^{-1}) in the dark at 25ºC with 30-day subculture intervals as described [12]. Transgenic callus lines were cultivated under the same conditions. The inoculum biomass was 200 mg (each callus was weighed using an electronic balance). Samples were harvested from 30 days cultures, weighed and used for RT-PCR. The calli were dried under a hot air flow (60°C for 5 h) and were then used for determination of resveratrol. Growth indexes were calculated as follows: $(W-W_0)/W_0$,

where W_0 is callus weight at the beginning of cultivation, and W is the resulting callus weight after 30 days of cultivation.

Plant transformation and callus line selection

The KJM1 and KJM2 AID domain mutants of the *A. thaliana* calcium dependent protein kinase gene CPK1 (AK1 isoform) (GenBank accession no. L14771) were used in this study. These mutations were engineered by oligonucleotide-directed site-specific mutagenesis by Harper et al. [16]. The KJM1 mutation (designated in this work as AtCPK1-Ca) converted wild-type AtCPK1 to the constitutively active, Ca^{2+}-independent form [16]. The KJM2 mutation (designated in this work as AtCPK1-Na) converted wild-type AtCPK1 to the non-active form [21].

Wild-growing plants of *V. amurensis* were collected from the southern Primorsky Region (near Vladivostok) and were identified by the Botany Department of the Institute of Biology and Soil Science. Transformation experiments were performed as previously described [22]. Young apical shoots of plants were inoculated with *Agrobacterium tumefaciens* containing either pART27/AtCPK1-Ca (active form) or pART27/AtCPK1-Na (non-active form) plasmids [11]. After transformation, the calli were cultivated for a 3-month period in the presence of 250 mg L^{-1} of cefotaxime to suppress bacterial growth. The selection of transgenic aggregates was carried out for 10 months using 100–200 mg L^{-1} of kanamycin sulfate.

RNA Isolation and cDNA Synthesis

Total RNA was isolated from *V. amurensis* cultures by LiCl method, as previously described [23]. Each sample of the resulting RNA was treated with 1 U of RNase-free DNase I (Sileks M, Russia) according to the manufacturer's protocol. Following digestion, DNase was removed from the solution using sorbent BlueSorb (Sileks M), and RNA was precipitated with 2 volumes of 96% ethanol. The resulting RNA pellet was washed with ice-cold 70% ethanol and

resuspended in 20 µl of DEPC-treated water. The RNA concentration and 28S/18S ratios were determined using an RNA StdSens LabChip® kit and an Experion™ Automated Electrophoresis Station (Bio-Rad Laboratories, Inc., USA) with Experion™ Software System Operation and Data Analysis Tools (version 3.0) following the manufacturer's protocol and recommendations. Samples with 28S/18S ribosomal RNA between 1.5–2.0 and an RNA Quality Indicator (RQI) above 9.0 were used for real-time PCR analysis.

The first strand of cDNA was synthesized from 2.5 µg of RNA using 0.5 ng of oligo-$d(T)_{15}$ primer. Solutions containing the RNA and primer were preheated (5 min at 72°C) and then cooled on ice. Reverse transcription was performed in a 50 µl volume containing 1X M-MLV buffer, 0.24 mM dNTP mix and 200 U M-MLV reverse transcriptase (Sileks M). The reaction was carried out for 1 h at 36°C, followed by 10 min at 72°C. The obtained cDNA samples were diluted 1:5 with nuclease-free water. As an additional negative control, we performed RT-RCR reactions with every RNA sample without adding the M-MLV enzyme (RNA-RT control).

Isolation of cDNA clones corresponding to *V. amurensis 4CL* genes

To amplify sequences corresponding to *4CL* genes, degenerate primers were designed according to the GenBank amino acid sequences from different plant species. The primer set 4CL-DegD 5′-TGY GTN YTN CCN ATG TTY CAY AT-3′ and 4CL-DegR 5′-GCY TCN GTC ATN CCR TAN CCY TG-3′ were designed using the amino acid sequences VLPMFH and QGYGMTE, which are conserved in 4-coumarate-CoA-ligases and flank a 279-bp fragment of *V. amurensis 4CL*. These conserved amino acid segments were chosen based on the alignment of known plant *4CL* genes from *Capsicum annuum* 4CL2(ACF17632), *Citrus sinensis* 4CL2 (XP_006474168), *Theobroma cacao* CL2 (XP_007014191), *Ricinus communis* 4CL1 (XP_002533186), *Nicotiana tabacum* 4CL1 (BAA21073), *V. vinifera* CL1 (XP_002272782), *Nekemias grossedentata* 4CL1 (AGO02172), *Cinnamomum osmophloeum* 4CL (AFG26323),

Solanum tuberosum 4CL2 (XP_006366277), *Ipomoea purpurea* 4CL (AHJ60263), *Populus trichocarpa* 4CL (XP_002324477), *S. tuberosum* 4CL2 (XP_006366955), *V. vinifera* 4CL7 (XP_002276353), *R. communis* 4CL (XP_002523698), *Cicer arietinum* 4CL7 (XP_004487067), *S. tuberosum* 4CL7 (XP_006340129), *Glycine max* 4CL7 (NP_001243292), *S. lycopersicum* 4CL (XP_004251107), *V. vinifera* 4CL (XP_002285920), *Morus notabilis* 4CL (XP_010094597), *V. vinifera* 4CL (AM428701), *V. vinifera* 4CL (XM_002269909).

Using RT-PCR with these primers and total RNA from *V. amurensis* cells, cDNA fragments of predicted lengths were amplified. These fragments were isolated from gels with a Glass Milk Kit (Sileks, Russia) and subcloned into a pTZ57R/T plasmid using the InsT/Aclone PCR Product Cloning Kit (Fermentas, Vilnius, Lithuania). The clones were amplified with M13 universal primers and sequenced as described earlier [23] at the Instrumental Centre of Biotechnology and Gene Engineering of IBSS FEB RAS using an ABI 3130 Genetic Analyzer (Applied Biosystems, Foster City CA, USA).

Rapid amplification of cDNA ends

To obtain full-length sequences of *V. amurensis 4CL* genes, we performed Rapid Amplification of cDNA Ends (RACE), using step-out PCR technology, according to [24] with modifications (see below). cDNA was synthesized from total RNA isolated from the RBH callus culture and subjected to 25 cycles of amplification, using the SMART cDNA Amplification Kit, according to the manufacturer's instructions (Clontech, CA, USA). In our modified protocol of RACE, we used the degenerate primers 4CL-DegD and 4CL-DegR in the first round of PCR instead of gene-specific primers. The use of these primers allowed for the simultaneous amplification of all expressed isoforms of *4CL*. The gene-specific primers used for real-time PCR were employed in the second round of RACE to obtain individual amplicons for each isoform of *4CL*. The fragments obtained by RACE were cloned into the plasmid pTZ57R/T (Fermentas) and sequenced.

PCR and real-time PCR analysis

To verify the presence of the transgenes in transformed *V. amurensis* cells, PCR was performed with cDNA samples obtained from the R, R-Ca and R-Na cultures. The gene-specific primer pairs used in the PCR analysis of *AtCPK1* expression were 5′-CGG TGA TCT TGA CTT TTC GT-3′ and 5′-CAA CAC CAA ACT CCT CAC AAG-3′. This primer set flanked a 581 bp fragment and spanned both the KJM1 and KJM2 mutation sites. The *AtCPK1* fragment amplified using these primer set was excised from the gel and sequenced.

Quantitative real-time PCR (qPCR) analysis were done using a Bio-Rad CFX96 Real-Time System (Bio-Rad Laboratories) with 2.5x SYBR green PCR master mix containing ROX as a passive reference dye (Syntol, Moscow, Russia). Reactions were performed in 25 μl of solution containing 300 nM of each primer, 1 μl of the diluted cDNA sample and 2.5 mM $MgCl_2$. All PCR reactions were performed under the following conditions: 5 min at 95°C, followed by 35 cycles of 15 s at 95°C and 30 s at 60°C in a 96-well reaction plate. Four biological replicates, resulting from four independent RNA extractions, were used for analysis, and three technical replicates were analyzed for each biological replicate. Non-template controls and RNA-RT controls were included in the analysis to verify the absence of contamination. The absence of non-specific products and primer-dimer artifacts in the samples was confirmed by melting curve analyses performed at the end of each run and by product visualization using electrophoresis on a 1% agarose gel stained with ethidium bromide.

For analysis of expression of *V. amurensis 4CL* genes the following primer pairs were used: *Va4CL1*, 5'–TAA GTA TAA GGT CAC AAT TGC–3' and 5'–CTT GGC GTT AGG GAG CTT GG–3'; *Va4CL2*, 5'–GGG CTT GCT GTG GTT ATG TG–3' and 5'–CTC CTC CAT CAA CTC CTT CC–3'; *Va4CL3*, 5'–CAA CGG TGG TGG TGC TCT CG–3' and 5'–CTT GGC CTT TAT TTT ATC AGC G–3'; *Va4CL4*, 5'–CCA CCA TAA CCG GCT AGA G–3' and 5'–CTC TAG CCG GTT ATG GTG G–3'; *Va4CL5*, 5'–GGG GAA GGA GCT GGA GGC GGC–3' and 5'–CGT CAA CAT CGA TGG TAG AG–3'.

For analysis of expression of *V. amurensis CDPK* genes the following primer pairs were used: *VaCDPK2* (GenBank accession no. KF042354) 5'-GAT TAT GGG GAG TTC ATA G 3'- and 5'-ACG CCT CTC TAA ACC CCA TAC-3'; *VaCDPK20* (GenBank accession no. KC488322) 5'-AGA CTA TGG TGA GTT TGT GG-3' and 5'-GTT ATT TTG TAT CCC TTC TTG-3'; *VaCDPK29* (GenBank accession no. KC488317) 5'-TTA TCT CTG CTT CCA CTC G-3' and 5'-TAA AGA CGC TGA TGG ATG CTG T-3'.

As a reference gene, we used *VaActin* (GenBank accession no. DQ517935). The primer set 5′-GTG CTG GAT TCT GGT GAT GG-3′ and 5′-CGT AGT CAA GAG CAA CAT ATG-3′ flanked a 217 bp fragment.

Primer efficiency of > 95% was confirmed with a standard curve spanning seven orders of magnitude. Data were analyzed, using CFX Manager Software (Version 1.5) (Bio-Rad Laboratories).

Molecular phylogenetic analysis

Sequences of plant 4CLs were retrieved from GenBank in a search carried out using the amino acid sequence of 4CLs from *V. amurensis* against the non-redundant protein database. GenBank sequences and sequences described in this work (in total 27) were aligned using the MUSCLE program [25] with default settings and refined manually. Phylogenetic tree was generated using the maximum-likelihood (ML) method of tree construction. Prior to the analysis, the ProtTest program v.2.4 [26] was used to determine the most appropriate amino acid substitutions that best fit the data. The best substitution matrix suggested by ProtTest was JTT+I+G+F. For the ML analysis, the Phyml program (v.3.0) was used [27] with the best substitution model suggested by ProtTest. Three hundred bootstrap cycles were carried out to obtain statistical support for the phylogeny.

Resveratrol content

Chemicals

All solvents were of high-performance liquid chromatography (HPLC) grade. Analytical standards: *trans*-resveratrol and *trans*-piceid were obtained from Sigma-Aldrich (St. Louis, MO, USA), *trans*-ε-viniferin was obtained from Panreac AppliChem (GmbH, Germany).

Sample preparation for analytical chromatography

The oven-dried (50°C to a constant weight) and powdered callus samples (100–200 mg) were extracted with methanol (the solid:liquid ratio was 1:30 w/v). The mixture was sonicated for 10 min, incubated for 4 h at 40°C (Environmental Shaker Incubator ES-20 biosan, Latvia), and then centrifuged (15000 g, 10 min). The supernatant was filtered, and the residue was re-extracted in the same manner. The extracts were combined and cleared with a 0.45-μm membrane (Millipore, Bedford, MA, USA), and 1–5 μL aliquots were used for HPLC analysis.

Analytical chromatography

HPLC coupled with UV and high-resolution mass spectrometry (HPLC-UV-HRMS) for the identification of stilbenes was performed using a LCMS-IT-TOF tandem ion-trap/time-of-flight mass-spectrometer (Shimadzu, Japan) equipped with a LC-20AD Prominence liquid chromatograph (Shimadzu, Japan) and a SPD-M20A photodiode array detector. An analytical Ascentis C18 column (100 mm, 2.1 mm i.d., 3 μm part size, Supelco, Bellefonte, Pennsylvania, USA) for separation was applied. All MS experiments were conducted using electrospray ionization (ESI) with simultaneous negative and positive ion detection The following settings were employed: the range of detection was 100–1,000 *m/z* with a resolution of 12,000, the drying gas (N2) pressure was 195 kPa, the nebulizer gas (N_2) flow rate was 1.5 L/min, the ion source potential changed from -3.8 to 4.5 kV, and the interface temperature was 200°C. The MS^2 data were obtained using argon as the collision ionization gas with pressure 0.003 Pa. The range of mass detection for the precursor ion fragments was 50–600 *m/z*. Separation was carried out under

the following conditions: the column temperature was 40°C, and the mobile phase consisted of 0.1 % aqueous acetic acid (A) and acetonitrile (B). The following elution gradient was used with a flow rate of 0.2 mL/min: 5 min 0 % B; 40 min 100 % B; and then eluent B for 50 min. UV spectra were recorded in the 190–400 nm range.

Quantitative analysis of stilbene derivatives by HPLC with UV (HPLC-UV) detection was performed using an Agilent Technologies 1260 Infinity LC system (Agilent Technologies, USA) equipped with a G1315D photodiode array detector, a G1311C quaternary pump with low-pressure gradient unit, a G1316A column oven and a G1329B autosampler. The extracts were separated on Zorbax C18 columns (150 mm, 2.1 mm i.d., 3.5 μm part size, Agilent Technologies, USA). The column temperature was 40°C. The mobile phase comprised of 0.1 % aqueous acetic acid (A) and acetonitrile (B). The following elution gradient was used with a flow rate of 0.25 mL/min: 0 min 0 % B; 17 min 45 % B; 27 min 100 % B; and then eluent B for 37 min. UV spectra were recorded in the range of 200–400 nm, and chromatograms were acquired at 310 nm. Quantitative determination of compounds found in the investigated samples was carried out using four-point regression curves, which were built with the existing standards.

Statistical analysis

All values are expressed as the mean ± SE. For comparison among multiple data points, analysis of variance (ANOVA) followed by a multiple comparison procedure was employed. Fisher's least significant difference (LSD) *post-hoc* test was employed for inter-group comparisons. All statistical calculations were performed with Statistica 10.0 (StatSoft Inc., USA). The level of statistical significance was set at $p < 0.05$.

Network visualization

The network was built using the program Cytoscape, version 2.8.3 [28] as previously described [29]. The data loaded into the program were obtained from the latest version of PAIR [PAIR-V3.3 [30]; http://www.cls.zju.edu.cn/pair/]. The protein-protein interactions presented in

PAIR were compared with the databases BioGRID [31] (http://thebiogrid.org/) and TAIR [32] (http://www.arabidopsis.org./). The size of each circle is correlated with the "betweenness centrality" metric, which describes the global position ("centrality") of the protein in the interactome. Betweenness centrality was automatically calculated by Cytoscape: the higher the value, the larger the circle.

Results

Transformation and growth of transgenic cultures

Transgenic calli V-Ca and V-Ca' (callus lines transformed with *AtCPK1-Ca*, a constitutively active, Ca^{2+}-independent form of the gene) as well as V-Na and V-Na' (callus lines transformed with *AtCPK1-Na*, a non-active form of the gene) were obtained via *Agrobacterium*-mediated transformation of *Vitis amurensis* wild-growing plants as described in the Materials and Methods. The selection of transgenic callus lines was achieved through ten passages on medium supplemented with kanamycin. During this time, the *AtCPK1-Na* transformed callus lines continued to grow as creamy-white calli, which did not vary from the control callus Va, whereas the *AtCPK1-Ca* transformed lines gradually began to form brown colored compact callus aggregates.

cDNAs were prepared from control and transgenic cell lines and PCR amplification with primers corresponding to *VaActin* was performed to confirm that the cDNA was native. Quantitative real-time PCR-based analysis showed that the *V. amurensis* calli, transformed with *AtCPK1-Ca* and *AtCPK-Na*, expressed *AtCPK1* gene sequences (Fig. 1A). The type of mutation in the auto-inhibitory domain of the *AtCPK1* gene in each callus culture was confirmed by sequencing.

The control and transgenic lines V-Na grew vigorously as friable tissues with similar color. The V-Ca cell lines formed brown compact callus aggregates (Fig. 1B). Investigation of the growth parameters of these cultures showed that the expression of the non-active form of *AtCPK1* in the V-Na did not significantly affect callus growth, but growth of the V-Ca lines was

significantly affected. Growth indexes were determined to be up to 18.0, 16.6 and 21.5 for the Va, V-Na and V-Ca lines, respectively. The dynamics of callus growth of the non-transgenic and transgenic cultures were similar and could be described by standard sigmoidal curves.

Identification of stilbenes

The results of the HPLC-UV-HRMS analysis of *V. amurensis* control cell cultures and the *AtCPK1*-transformed cultures V-Na and V-Ca (Fig. 2A, Fig. 3) showed the presence of five components with maximum UV adsorption at 305-327 nm. Similar UV characteristics are typical for *trans* isomers of stilbenes [33, 34, 35]. The UV spectra of components **1**-**3** were identical to *trans*-resveratrol, and the UV spectra of components **4**-**5** were similar to *trans*-resveratrol dehydrodimers (commonly known as viniferins). All chromatographic and MS characteristics of components **2**–**4** (Table 1, Fig. 2) corresponded to the MS data of standard compounds and the literature [34, 35, 36]. The detailed MS investigation allowed us to identify components **1** and **5**, standards of which were not available.

Component **1** showed MS data (Table 1, Fig. 2B) that corresponded to previously described resveratrol di-glucoside [37, 38]. On the negative MS^2 spectrum of component **1** (precursor ions with *m/z* 551.1771), two types of ion signals were observed. The ions with *m/z* 389.1236 and 227.0708 corresponded to fragments produced by the consistent elimination of one or two dehydrated molecules of hexose. The positive MS^2 spectrum (precursor ions with *m/z* 553.1918) showed fourteen fragment ions. More intensive ions with *m/z* 391.1396 and 229.0867 corresponded to fragments formed by the loss of one and two dehydrated molecules of hexose. Other fragment ions with *m/z* 373.1288, 355.1180 and 337.1076, were formed by the loss of one hexose molecule coupled with the loss of one, two or three molecules of water, respectively. In addition, ions with *m/z* 535.1817, 517.1711 and 499.1603 (formed by the loss of H_2O, 2 H_2O and 3 H_2O, respectively) were observed in the positive MS^2 spectrum. This type of *trans*-resveratrol di-glucoside was described early in *V. vinifera* cell suspension cultures [37].

The results of molecular formula calculations based on high-resolution mass spectrometry for components **4** and **5** (Table 1, Fig. 2) demonstrated an elemental composition typical for resveratrol dehydrodimers ($C_{28}H_{22}O_6$). These isomers were identified by tandem mass spectrometry. The MS^2 spectra of the quasi-molecular ions ($[M+H]^+$ and $[M-H]^-$) of components **4** and **5** showed similar patterns of fragmentation, but there were significant differences. For example, the negative MS^2 spectra of both compounds were characterized by the presence of ion signals with *m/z* 435.124 (due to the loss of water molecules), ion signals with *m/z* 359.093 (consistent with the loss of one phenolic moiety), ion signals with *m/z* 369.113 (consistent with the loss of the neutral fragment $C_4H_4O_2$ due to degradation of the dihydroxy-substituted benzene moiety), and ion signals with *m/z* 411.124 (consistent with the loss of the neutral fragment C_2H_2O). Signals of ions with *m/z* 359.093 had a lower intensity in the spectrum of component **5** than in the spectrum of component **4**. This finding indicated the presence of a single phenolic moiety in the molecular structure of component **5**. Signals of ions with *m/z* 369.113, 411.124 and 435.124 had a higher intensity in the spectrum of component **5** than in the spectrum of component **4**. The fragmentation pattern of the negative quasi-molecular ions of component **5** corresponded to previously described *trans*-δ-viniferin [34, 35, 39].

Content of *trans*-resveratrol di-glucoside, *trans*-piceid, *trans*-resveratrol, *trans*-ε-viniferin and *trans*-δ-viniferin in control and *AtCPK*-transformed callus cultures of *V. amurensis*

All cultures produced five major stilbenes: *trans*-resveratrol di-glucoside, *trans*-piceid, *trans*-resveratrol, *trans*-ε-viniferin and *trans*-δ-viniferin. As shown in Fig. 4, transformation with the non-active *AtCPK1* gene did not cause changes in stilbene content in transgenic calli V-Na' and V-Na compared to non-transformed culture. Stilbene content was not more than 0.5 mg/g DW in these cultures. Transformation of plants with the constitutively active form of *AtCPK1* increased the levels of *trans*-resveratrol di-glucoside, *trans*-piceid, *trans*-resveratrol, *trans*-ε-viniferin and *trans*-δ-viniferin by 1.3-9-fold and *trans*-resveratrol by 22-157-fold in the V-Ca'

and V-Ca cell cultures, respectively (Fig. 4). Correspondingly, the resveratrol content increased up to 0.45 % of the dry wt. The most productive lines, V-Na and V-Ca, were selected for further analysis.

Resveratrol production by Va, V-Na and V-Ca calli

Va, V-Na and V-Ca callus cultures possessed active growth because biomass production of all callus lines was more than 300 g L^{-1} fresh weight (Table 2). Transformation of cells with the constitutively active form of *AtCPK1* significantly increased this parameter, bringing the biomass accumulation to 576 g L^{-1} fresh weight (Table 2). The Va and V-Na cell lines accumulated ~ 0.005% dry wt. of resveratrol, and the resveratrol production of these cell lines did not exceed 0.6 mg L^{-1}. Transformation of grape plants with the constitutively active form of *AtCPK1* dramatically increased the resveratrol accumulation compared to the other cell cultures. Resveratrol production in the V-Ca cultures reached 69.7 mg L^{-1}, 135-fold greater than the resveratrol production of the control calli (Table 2).

Identification and amino acid analysis of the *4CL* genes *of V. amurensis*

To identify *V. amurensis* 4-coumarate-CoA ligase (*4CL*) transcripts, PCR reactions were performed with degenerate primers corresponding to conserved parts of known plant 4CLs and cDNA samples obtained from *V. amurensis* callus cultures. Fragments of the predicted lengths were obtained and cloned separately into the pTZ57R/T vector. A total of 118 cDNA clones were randomly sequenced, of which five *Va4CL* genes of *V. amurensis* (*Va4CL1*-*Va4CL5*) were identified. To recover full-length cDNAs, RACE PCR was performed and the complete sequences of the *Va4CL1*, *Va4CL2*, *Va4CL3*, *Va4CL4* and *Va4CL5* transcripts were determined and submitted to GenBank under the accession numbers KX276191, KX276192, KX276193, KX276194 and KX276195, respectively. High levels of amino acid identity were found between the deduced V. *amurensis* 4CLs and known 4CL enzymes from other plants, using the BLAST algorithm (Table 3).

Phylogenetic analysis

We further performed the phylogenetic analysis based on 4CLs from *V. amurensis* and from other plants by applying the maximum-likelihood method (Fig. 5). Additional analysis using maximum parsimony and neighbor-joining methods of tree reconstruction yielded very similar results, thus confirming the reliability of the obtained results. A total of 26 4CL sequences from 6 plant species (*V. amurensis, V. vinifera, N. tabacum, A. thaliana, G. max* and *R. communis*) were used in this analysis. The unrooted phylogenetic tree categorized the 4CLs proteins into four groups with high bootstrap values (Fig. 5). The first group includes proteins which belong to class I of the true 4CLs [40]. These 4CLs are associated with lignin biosynthesis in the unstressed plant cells [41]. The second group comprises class II of the true 4CLs [40] which are activated in stressed cells and involved in the biosynthesis of phenylpropanoids [41]. Group III and group IV includes proteins collectively called 4CL-like enzymes [42], which are involved in the biosynthesis of jasmonic acid [43].

The *AtCPK* increases resveratrol accumulation via activation of *4CL* genes expression

Next, we assessed the impact of *AtCPK1* on *Va4CL1-5* gene expression in control and transgenic *V. amurensis* calli using quantitative real-time PCR analysis. Our results show that overexpression of *AtCPK1-Na* did not have any effect on the expression of *Va4CL* genes compared to control cells (Fig. 6). At the same time *AtCPK1-Ca* significantly increased the expression of all *Va4CLs* but to different extents. Expression of *Va4CL3*, *Va4CL4* and *Va4CL5* in *AtCPK1-Ca*-transgenic calli was 18, 3 and 27 times higher, respectively, in comparison with both control and *AtCPK1-Na*-transgenic callus lines. Analysis of *Va4CL1* and *Va4CL2* has shown nearly 7-fold increase in transcript abundance in the transgenic cell line expressing the constitutively active form of the *AtCPK1* gene. It should be noted, that among *V. amurensis 4CLs*, *Va4CL1* and *Va4CL2*, were expressed 4-35 times higher than other isoforms in both control and *AtCPK1-Na*-transgenic callus lines. These isoforms together with *VaCL3* were also predominant *4CL* transcripts expressed in *AtCPK1-Ca*-transgenic calli.

The *AtCPK* does not affect the expression of *V. amurensis* homologous *CDPK* genes

In order to estimate the effect of heterologous expression of *AtCPK1* mutant forms on endogenous *V. amurensis CDPK* isoforms, we analyzed expression levels of the *VaCDPK2*, *VaCDPK20* and *VaCDPK29* genes, which show 77%, 73% and 62% identity with AtCPK1 at the amino acid level, respectively. *VaCDPK20* gene showed the highest level of expression compared to other analyzed *VaCDPK* isoforms; *VaCDPK29* isoform possessed the lowest level of expression in all samples (Fig. 7). No significant changes were observed in *VaCDPKs* mRNA expression levels in control and *AtCPK1*-transgenic cell cultures of *V. amurensis* (Fig. 7).

Discussion

In this work, we report the establishment of *AtCPK1-Ca*-transformed callus cultures of *Vitis amurensis* in which the production of resveratrol was activated 137-fold compared to non-transformed calli, as well as calli transformed with the non-active *AtCPK1* gene. The levels of other stilbenes (*trans*-resveratrol di-glucoside, *trans*-piceid, *trans*-resveratrol, *trans*-ε-viniferin and *trans*-δ-viniferin) were also significantly increased in the *AtCPK1-Ca*-transformed cell cultures. Another important effect of transformation was the increase in callus biomass of up to 70%.

The activation of anthraquinone production by the *AtCPK1-Ca* gene [11] and the activation of stilbene production described in this paper indicate that *CDPKs* could have a general role in the activation of plant secondary metabolic processes. Indeed, anthraquinones and polyphenols represent distinct classes of secondary metabolites of different pathways with different entry enzymes. The simplest explanation of the effect of *CPK1* might be the non-specific activation of secondary metabolism by oxidative burst, mediated by the well-known interaction of CDPKs with NADPH oxidases [44]. This explanation could be strengthened if we could observe cell growth inhibition via expression of the *CPK1* gene. However, the growth of our *AtCPK1-Ca*-transgenic cultures was even more active than that of the control cultures (Table 2). Here we observe the interesting phenomenon of growth activation by kinases again. It was

shown previously that *CDPK1* from ginger promoted salinity and drought stress tolerance by improving growth [45], overexpression of *VaCPK20* or *VaCPK29* in *V. amurensis* calli increased resveratrol content and fresh biomass accumulation [46, 47]. It should be noted, however, that the native form of *AtCPK1* overexpressed in *Rubia codifolia* cells did not lead to an increase in callus biomass [22], while constitutively active *AtCPK1* even slightly inhibited the growth by 9-15% [11]. The latter effect may be associated with the competition between growth and production of anthraquinones in *R. cordifolia* cells. Similar phenomenon was observed in *Morinda citrifolia* suspension culture in which cell division was inhibited in high-anthraquinone-producing lines [48]. Perhaps, a combination and interaction of various factors can affect growth modulation by *AtCPK1* and their precise mechanism of action is presently unclear.

4-Coumarate:coenzyme A ligase (4CL) plays a key role in synthesis of phenylpropanoid derivatives including the formation of resveratrol [49]. Overexpression of *4CL* from tobacco and stilbene synthase (STS) from grapes in *Saccharomyces cerevisiae* and *Escherichia coli* caused to resveratrol accumulations in the culture medium in 16 mg/liter and 6 mg/liter for *E. coli* and yeast, respectively [5]. Although the transcriptional regulation of *STS* gene expression involved in resveratrol biosynthesis in *V. amurensis* was previously investigated [46], functional analysis of *4CL*s remain largely unknown. In this report, we studied the effect of the *AtCPK1* gene on *4CL* gene expression. The sequences of the *4CL* genes from *V. amurensis*, *Va4CL1*, *Va4CL2*, *Va4CL3*, *Va4CL4* and *Va4CL5*, were identified and deposited to GenBank. Differential expressions of *Va4Cl* genes in control, *AtCPK1-Na*- and *AtCPK1-Ca*-transgenic calli were investigated by real-time PCR. In accordance with our assumption, expression of the *AtCPK1-Na* gene caused no significant perturbations in *Va4CL* genes expression. The overexpression of the *AtCPK1-Ca* gene caused a significant upregulation of all studied *4CL* genes. Notably, that among *V. amurensis 4CLs*, *Va4CL1* and *Va4CL5*, which are potentially involved in lignin production and biosynthesis of stilbenoids, respectively, were significantly more activated (2.5-9 times higher) than other isoforms.

To investigate whether foreign *CDPK* could affect the expression of endogenous *V. amurensis CDPK* genes, we analyzed transcriptional levels of the *VaCDPK2*, *VaCDPK20* and *VaCDPK29* genes, which show high levels of identity with *AtCPK1*. No significant changes were observed in *VaCDPKs* mRNA expression levels in control and *AtCPK1*-transgenic cell cultures of *V. amurensis*, thus indicating no impact of the *VaCDPK2*, *VaCDPK20* and *VaCDPK29* is to be expected.

The literature data suggests that *AtCPK1* activates expression of numerous genes related to defense and stress responses in the absence of pathogen challenge [19]. Among them were several PR genes, plant defensin and lipid transfer protein genes. *AtCPK1* also controls the expression levels of genes implicated in regulation of oxidative stress, such as respiratory burst oxidase protein B, glutathione-S-transferases, peroxidases, glutaredoxins and thioredoxins. The *PAD3* and *PAD4* genes encoding enzymes involved in the biosynthetic pathway for production of the camalexin were also activated. However, information about regulatory components that mediates such complex reactions is lacked.

In this case, it is important to look at the complex signaling pathways mediated by CPK1. To reconcile these links, we constructed the CPK1-based sub-network of protein-protein interactions in *Arabidopsis* (Fig. 8). Signaling modules regulating reactive oxygen species (ROS) and stress resistance are easily distinguishable and can be affected by CPK1 interactions with SOS2 and CIPK15, where a clear link between CPK1 and the signaling component SOS3-SOS2/CBL1-CIPK15-NDPK2 [50] is observed. CPK1 also interacts with 14-3-3 proteins (general regulatory proteins, GRFs). Links between secondary metabolic regulator modules and GRFs (each forms a branched chain of protein-protein interactions) are presently unknown [29]. However, such a link is possible by CPK1-GRF2-WRKYs (WRKY DNA-binding proteins) interactions. Additionally, the CPK1-GRF2-DHS1 (3-deoxy-D-arabino-heptulosonate 7-phosphate synthase 1) interaction may be involved in the activation of biosynthesis of stilbene precursors, such as chorismate (see also http://thebiogrid.org/15439/summary/arabidopsis-thaliana/dhs1.html).

The CPK1-ERS2 interaction provides link with ethylene signaling, i.e. the connection with ethylene-responsive modules, which in turn participate in secondary metabolism regulation [29, 51]. Note that links with MYB or bHLH transcription factors, which activate secondary metabolism in *Arabidopsis*, were not detected by our analysis. This finding means that secondary metabolism activation by CPK1 is most likely an indirect process and is a part of general stress-mediated defense reactions activated by *AtCPK1*. Whether these reconstructions are valid for *Vitis* or other plant species will be the subject of further experimental studies. Our reconstruction shows that the most related kinase to CPK1 is CPK10. These protein kinases are phylogenetically unrelated but possess similar functions [17]. The functional similarity of CPK1 and CPK10 is evident because these kinases have several common targets (Fig. 8). Therefore, the *AtCPK10* gene is also promising for bioengineering purposes.

Acknowledgments

The analyses described in this work were performed using equipment from the Instrumental Centre for Biotechnology and Gene Engineering at the Institute of Biology and Soil Science. Financial support was provided by the Russian Science Foundation (Grant no. 14-14-00230).

"Financial support was provided by the Russian Science Foundation (RSF ?14-14-00230) for the generation of transgenic cultures, cloning, sequencing, real-time detection of gene expression and by the RF President's grant for young scientists (??-491.2017.4) for determination of composition and quantity of stilbenes and preparation of the article" instead of "Financial support was provided by the Russian Science Foundation (Grant no. 14-14-00230)".

References

[1] Palsamy P, Subramanian S. Resveratrol, a natural phytoalexin, normalizes hyperglycemia in streptozotocin-nicotinamide induced experimental diabetic rats. Biomed Pharmacother 2008; 62:598–605.

[2] Agrawal M. Natural polyphenols based new therapeutic avenues for advanced biomedical applications. Drug Metab Rev 2015; 3:1–11.

[3] Ourtoule J-C, Bourhis M, Vercauteren J, Théodore N. First symmetrical bicyclo[6.6.0]tetradecane resveratrol tetramer from stalks of *Vitis vinifera* (Vitaceae). Tetrahedron Lett 1996; 37:4697–4700.

[4] Mattarei A, Biasutto L, Romio M, Zoratti M, Paradisi C. Synthesis of resveratrol sulfates: turning a nightmare into a dream. Tetrahedron 2015; 71:3100–3106.

[5] Beekwilder J, Wolswinkel R, Jonker H, Hall R, de Vos CH, Bovy A. Production of resveratrol in recombinant microorganisms. Appl Environ Microbiol 2006; 72:5670-5672.

[6] Jeandet P, Clément C, Courot E. Resveratrol production at large scale using plant cell suspensions. Eng. Life Sci 2014; 14:622–632.

[7] Sparvoli F, Martin C, Scienza A, Gavazzi G, Tonelli C. Cloning and molecular analysis of structural genes involved in flavonoid and stilbene biosynthesis in grape (*Vitis vinifera* L.). Plant Mol Biol 1994; 24:743–755.

[8] Afonso M, Ferreira S, Domingues F, Silva F. Resveratrol production in bioreactor: Assessment of cell physiological states and plasmid segregational stability. Biotechnol Rep 2015; 5:7–13.

[9] Delaunois B, Cordelier S, Conreux A, Clément C, Jeandet P. Molecular engineering of resveratrol in plants. Plant Biotechnol J 2009; 7:2–12.

[10] Zhao J, Davis LC, Verpoorte R. Elicitor signal transduction leading to production of plant secondary metabolites. Biotechnol Adv 2005; 23:283–333.

[11] Shkryl YN, Veremeichik GN, Bulgakov VP, Zhuravlev YN. Induction of anthraquinone biosynthesis in *Rubia cordifolia* cells by heterologous expression of a calcium-dependent protein kinase gene. Biotechnol Bioeng 2011; 108:1734–1738.

[12] Bulgakov VP, Gorpenchenko TY, Shkryl YN, Veremeichik GN, Mischenko NP, Avramenko TV, Fedoreyev SA, Zhuravlev YN. CDPK-driven changes in the intracellular ROS level and plant secondary metabolism. Bioeng Bugs 2011; 2:327–330.

[13] Chen J, Xue B, Xia X, Yin W. A novel calcium-dependent protein kinase gene from *Populus euphratica* confers both drought and cold stress tolerance. Biochem Biophys Res Commun 2013; 441:630–636.

[14] Hegeman AD, Rodriguez M, Han BW, Uno Y, Phillips GN Jr, Hrabak EM, Cushman JC, Harper JF, Harmon AC, Sussman MR. A phyloproteomic haracterization of *in vitro* autophosphorylation in calcium-dependent protein kinases. Proteomics 2006; 6:3649–3664.

[15] Wernimont AK, Artz JD, Finerty P Jr, Lin YH, Amani M, Allali-Hassani A, Senisterra G, Vedadi M, Tempel W, Mackenzie F, Chau I, Lourido S, Sibley LD, Hui R. Structures of apicomplexan calcium-dependent protein kinases reveal mechanism of activation by calcium. Nat Struct Biol 2010; 17:596–601.

[16] Harper JF, Huang JF, Lloyd SJ. Genetic identification of an autoinhibitor in CDPK, a protein kinase with a calmodulin-like domain. Biochemistry 1994; 33:7267–7277.

[17] Sheen J. Ca^{2+}-dependent protein kinases and stress signal transduction in plants. Science 1996; 274(5294):1900–1902.

[18] Dammann C, Ichida A, Hong B, Romanowsky SM, Hrabak EM, Harmon AC, Pickard BG, Harper JF. Subcellular targeting of nine calcium-dependent protein kinase isoforms from *Arabidopsis*. Plant Physiol 2003; 132:1840–1848.

[19] Coca M, San Segundo B. AtCPK1 calcium-dependent protein kinase mediates pathogen resistance in Arabidopsis. Plant J 2010; 63:526–540.

[20] Xing T, Wang X-J, Malik K, Miki B. Ectopic expression of an *Arabidopsis* calmodulin-like domain protein kinase-enhanced NADPH oxidase activity and oxidative burst in tomato protoplasts. Mol Plant Microbe Interact 2001; 14:1261–1264.

[21] Huang JF, Teyton L, Harper JF. Activation of a Ca(2+)-dependent protein kinase involves intramolecular binding of a calmodulin-like regulatory domain. Biochemistry 1996; 35:13222–13230.

[22] Shkryl YN, Veremeichik GN, Makhazen DS, Silantieva SA, Mishchenko NP, Vasileva EA, Fedoreyev SA, Bulgakov VP. Increase of anthraquinone content in *Rubia cordifolia* cells transformed by native and constitutively active forms of the *AtCPK1* gene. Plant Cell Rep 2016; 35:1907–1916.

[23] Veremeichik GN, Shkryl YN, Pinkus SA, Bulgakov VP. Expression profiles of calcium-dependent protein kinase genes (*CDPK1–14*) in *Agrobacterium rhizogenes* pRiA4-transformed calli of *Rubia cordifolia* under temperature- and salt-induced stresses. J Plant Physiol 2014; 171:467–474.

[24] Matz M, Shagin D, Bogdanova O, Lukyanov S, Diatchenko L, Chenchik A. Amplification of cDNA ends based on template-switching effect and step-out PCR. Nucleic Acids Res 1999; 2:1558–1560.

[25] Edgar R. MUSCLE: multiple sequence alignment with high accuracy and high throughput. Nucleic Acids Res 2004; 32:1792–1797.

[26] Abascal F, Zardoya R, Posada D. ProtTest: selection of best-fit models of protein evolution. Bioinformatics 2005; 21:2104–2105.

[27] Guindon S, Gascuel O. A simple, fast, and accurate algorithm to estimate large phylogenies by maximum likelihood. Syst Biol 2003; 52:696–704.

[28] Shannon P, Markiel A, Ozier O, Baliga NS, Wang JT, Ramage D, Amin N, Schwikowski B, Ideker T. Cytoscape: A software environment for integrated models of biomolecular interaction networks. Genome Res 2003; 13:2498–2504.

[29] Bulgakov VP, Avramenko TV, Tsitsiashvili GSh. Critical analysis of protein signaling networks involved in the regulation of plant secondary metabolism: focus on anthocyanins. Crit Rev Biotechnol 2016; 24:1–16.

[30] Lin M, Zhou X, Shen X, Mao C, Chen X. The predicted *Arabidopsis* interactome resource and network topology-based systems biology analyses. Plant Cell 2011; 23:911–922.

[31] Stark C, Breitkreutz BJ, Reguly T, Boucher L, Breitkreutz A, Tyers M. BioGRID: A general repository for interaction datasets. Nucleic Acids Res 2006; 34 (Database issue): D535–D539.

[32] Swarbreck D, Wilks C, Lamesch P, Berardini TZ, Garcia-Hernandez M, Foerster H, Li D, Meyer T, Muller R, Ploetz L, Radenbaugh A, Singh S, Swing V, Tissier C, Zhang P, Huala E. The Arabidopsis Information Resource (TAIR): Gene structure and function annotation. Nucleic Acids Res 2008; 36 (Database issue): D1009–D1014.

[33] Trela BC, Waterhouse AL. Resveratrol: isomeric molar absorptivities and stability. J Agric Food Chem 1996; 44:1253–1257.

[34] Pezet R, Perret C, Jean-Denis JB, Tabacchi R, Gindro K, Viret O. δ-Viniferin, a resveratrol dehydrodimer: one of the major stilbenes synthesized by stressed grapevine leaves. J Agric Food Chem 2003; 51:5488–5492.

[35] Mulinacci N, Innocenti M, Santamaria AR, la Marca G, Pasqua G. High-performance liquid chromatography/electrospray ionization tandem mass spectrometric investigation of stilbenoids in cell cultures of *Vitis vinifera L.*, cv. Malvasia. Rapid Commun Mass Spectrom 2010; 24:2065–2073.

[36] Szewczuk LM, Forti L, Stivala LA, Penning TM. Resveratrol is a peroxidase-mediated inactivator of COX-1 but not COX-2: a mechanistic approach to the design of COX-1 selective agents. J Biol Chem 2004; 279:22727–22737.

[37] Larronde F, Richard T, Delaunay JC, Decendit A, Monti JP, Krisa S, Mérillon JM. New stilbenoid glucosides isolated from *Vitis vinifera* cell suspension cultures (cv. Cabernet Sauvignon). Planta Med 2005; 71:888–890.

[38] Jerkovic V, Nguyen F, Nizet S, Collin S. Combinatorial synthesis, reversed-phase and normalphase high-performance liquid chromatography elution data and liquid chromatography/positive atmospheric pressure chemical ionization tandem mass spectra of methoxylated and glycosylated resveratrol analogues. Rapid Commun Mass Spectrom 2007; 21:2456–2466.

[39] Szewczuk LM, Lee SH, Blair IA, Penning TM. Viniferin formation by COX-1: evidence for radical intermediates during co-oxidation of resveratrol J Nat Prod 2005; 68:36–42.

[40] Ehlting J, Büttner D, Wang Q, Douglas CJ, Somssich IE, Kombrink E. Three 4-coumarate:coenzyme A ligases in *Arabidopsis thaliana* represent two evolutionarily divergent classes in angiosperms. Plant J 1999; 19:9–20.

[41] Hamberger B, Hahlbrock K. The 4-coumarate:CoA ligase gene family in *Arabidopsis thaliana* comprises one rare, sinapate-activating and three commonly occurring isoenzymes. Proc Natl Acad Sci USA 2004; 101:2209–2214.

[42] Schneider K, Kienow L, Schmelzer E, Colby T, Bartsch M, Miersch O, Wasternack C, Kombrink E, Stuible H-P. A new type of peroxisomal acyl-coenzyme a synthetase from *Arabidopsis thaliana* has the catalytic capacity to activate biosynthetic precursors of jasmonic acid. J Biol Chem 2005; 280:13962–13972.

[43] Kienow L, Schneider K, Bartsch M, Stuible H-P, Weng H, Miersch O, Wasternack C, Kombrink E. Jasmonates meet fatty acids: functional analysis of a new acyl-coenzyme A synthetase family from *Arabidopsis thaliana*. J Exp Bot 2008; 59:403–419.

[44] Kobayashi M, Yoshioka M, Asai S, Nomura H, Kuchimura K, Mori H, Doke N, Yoshioka H. StCDPK5 confers resistance to late blight pathogen but increases susceptibility to early blight pathogen in potato via reactive oxygen species burst. New Phytol 2012; 196:223–237.

[45] Vivek P, Tuteja N, Soniya E. CDPK1 from ginger promotes salinity and drought stress tolerance without yield penalty by improving growth and photosynthesis in *Nicotiana tabacum*. PLoS One 2013; 8:e76392.

[46] Aleynova-Shumakova OA, Dubrovina AS, Manyakhin AY, Karetin YA, Kiselev KV. *VaCPK20* gene overexpression significantly increased resveratrol content and expression of stilbene synthase genes in cell cultures of *Vitis amurensis* Rupr. Appl Microbiol Biotechnol 2014; 98:5541–5549.

[47] Aleynova OA, Dubrovina AS, Manyakhin AY, Karetin YA, Kiselev KV. Regulation of resveratrol production in *Vitis amurensis* cell cultures by calcium-dependent protein kinases. Appl Biochem Biotechnol 2015; 175:1460–1476.

[48] van der Plas LHV, Eijkelboom C, Hagendoorn MJM. Relation between primary and secondary metabolism in plant cell suspensions. Plant Cell Tiss Org 1995; 43:111–116.

[49] Dixon R, Paiva N. Stress-induced phenylpropanoid metabolism. Plant Cell 1995; 7:1085–1097.

[50] Guo Y, Halfter U, Ishitani M, Zhu JK. Molecular characterization of functional domains in the protein kinase SOS2 that is required for plant salt tolerance. Plant Cell 2001; 13:1383–1400.

[51] Wang J, Wang Y, Yang J, Ma C, Zhang Y, Ge T, Qi Z, Kang Y. *Arabidopsis ROOT HAIR DEFECTIVE3* is involved in nitrogen starvation-induced anthocyanin accumulation. J Integr Plant Biol 2015; 57:708–721.

Figure legends

Fig. 1. The *AtCPK1* gene expression (A) and penotypes of transgenic *Vitis amurensis* callus cultures (A). Data from real-time, quantitative PCR (mean ± standard error) represent measurements of three independent replicates from two different RNA isolations and are presented as relative expression levels normalized to the expression of the *V. vinifera* actin gene. Different letters above the bars indicate statistically significant differences of means ($P < 0.05$), Fisher's LSD. Va, untransformed callus line; V-Na and V-Na', callus lines transformed with non-active *AtCPK1*, V-Ca and V-Ca', callus lines transformed with constitutively active *AtCPK1*. Cultures were grown for 4 weeks on $W_{B/A}$ medium.

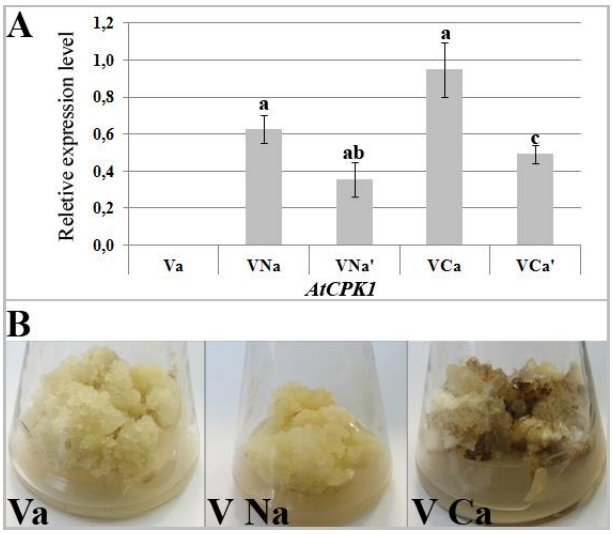

Fig. 2. HPLC-UV-HRMS identification of stilbenes in methanolic extracts of studied samples: A, chromatogram recorded at 310 nm; B, overlapping of the extracted ion chromatograms acquired in negative ion mode. The monitored ions correspond to the most abundant deprotonated molecules $[M-H]^-$, using a restricted window of ± 0.0100 *m/z* unit centred on each selected ion. Peak numbers correspond to those shown in Table 1 and Fig. 3.

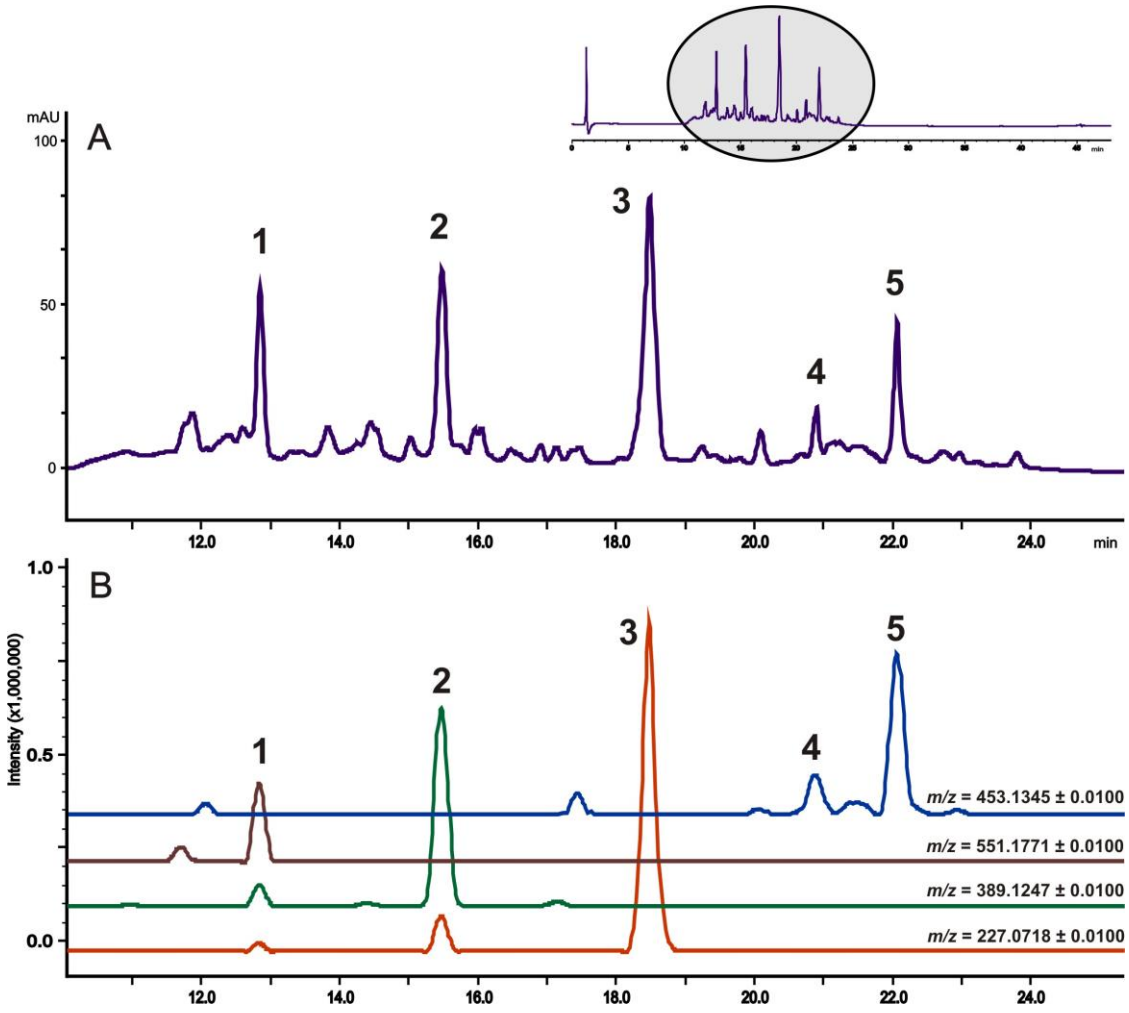

Fig. 3. UV spectra of stilbene derivatives identified in studied samples. Each spectrum was obtained from the top of the peak of the investigated component using a photodiode array detector. Spectrum numbers correspond to peak numbers shown in Table 1 (MS), Fig. 2 and Fig. 3.

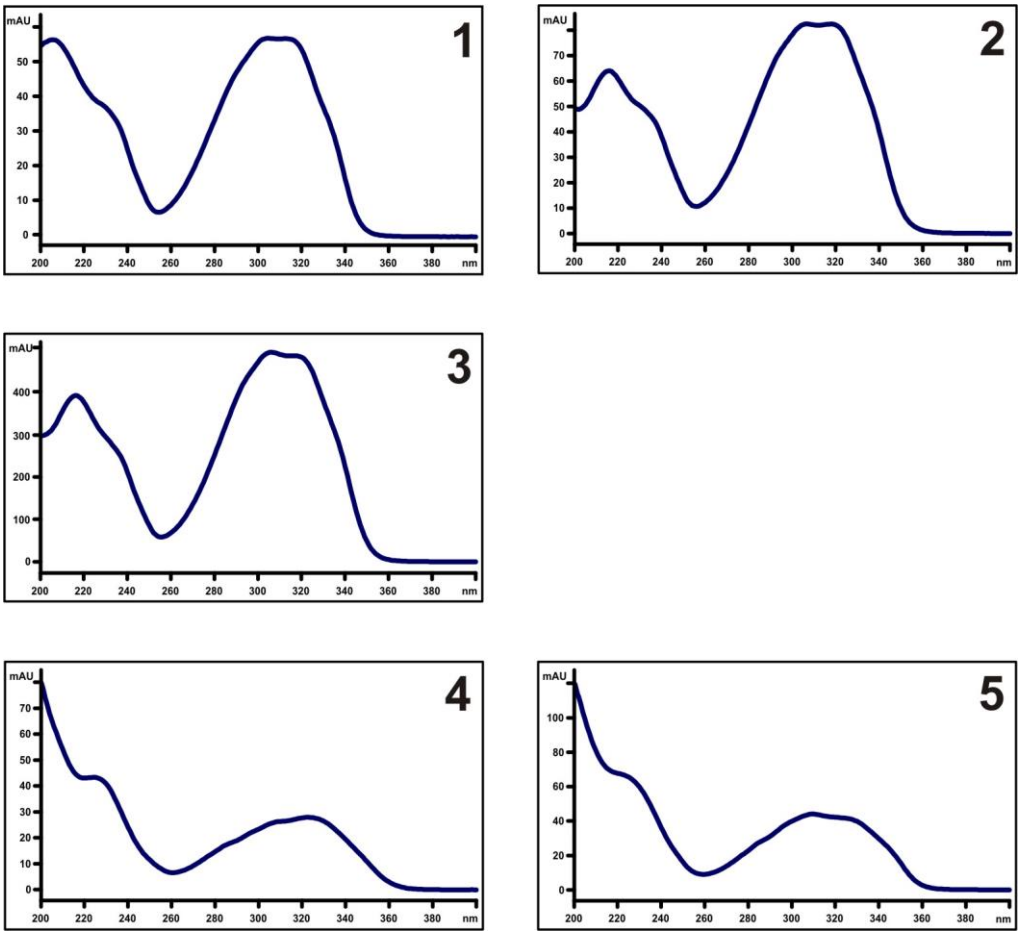

Fig. 4. Content of stilbenes (*trans*-resveratrol di-glucoside, *trans*-piceid, *trans*-resveratrol, *trans*-ε-viniferin and *trans*-δ-viniferin) in the control calli (Va), *AtCPK1-Na*-transformed callus cultures (V-Na and V-Na') and *AtCPK1-Ca*-transformed callus cultures (V-Ca and C-Ca'). Data are presented as mean ± standard error from four subcultures (biological replicates) with two technical replicates for each experiment. Different letters above the bars indicate significantly different means ($P < 0.05$), Fisher's LSD.

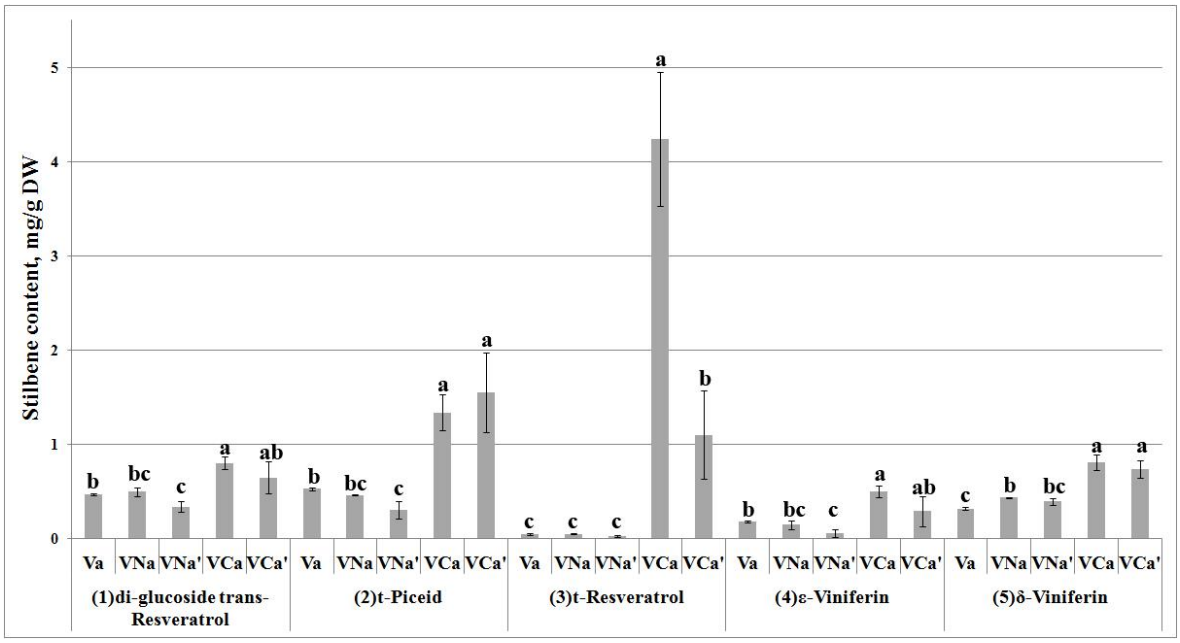

Fig. 5. Phylogenetic relationship among 4CL proteins from *V. amurensis*, *V. vinifera*, *N. tabacum*, *A. thaliana*, *G. max* and *R. communis* based on maximum-likelihood estimation. GenBank accession numbers of the proteins are given after the gene names. The four groups are marked from I to IV. The numbers on the branches represent bootstrap values.

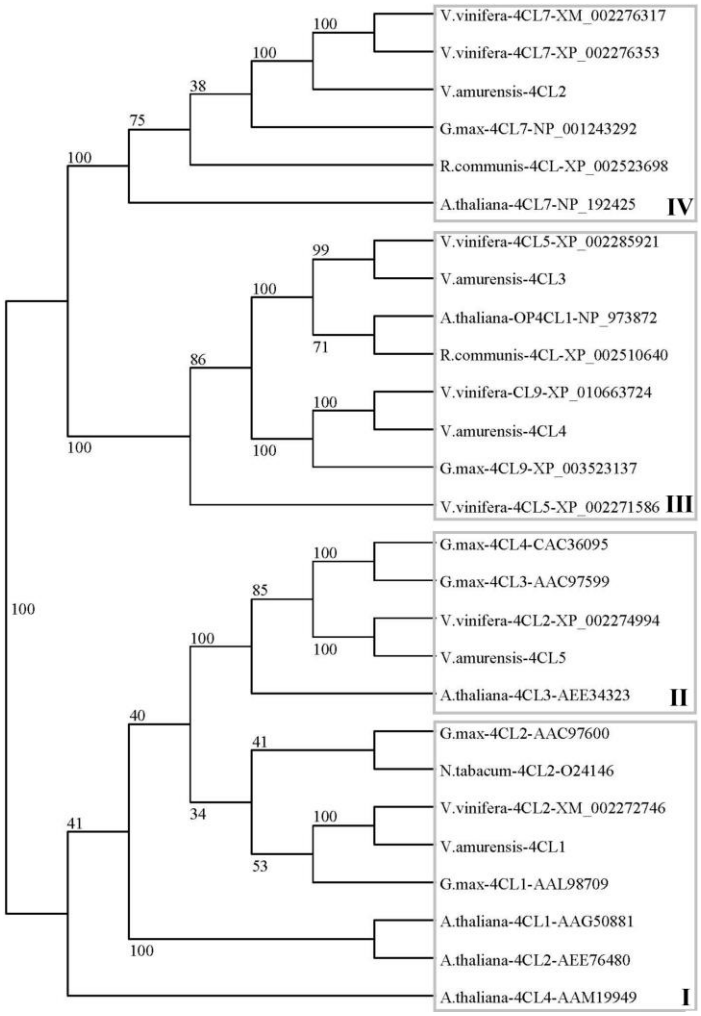

Fig. 6. Expression of *V. amurensis 4CL* genes in control callus culture (Va), callus line transformed with non-active *AtCPK1* (VNa) and callus line transformed with constitutively active *AtCPK1* (VCa). Data (mean ± standard error) represent measurements of three independent replicates from two different RNA isolations and are presented as relative expression levels normalized to the expression of the *V. vinifera* actin gene. Different letters above the bars indicate statistically significant differences of means ($P < 0.05$), Fisher's LSD.

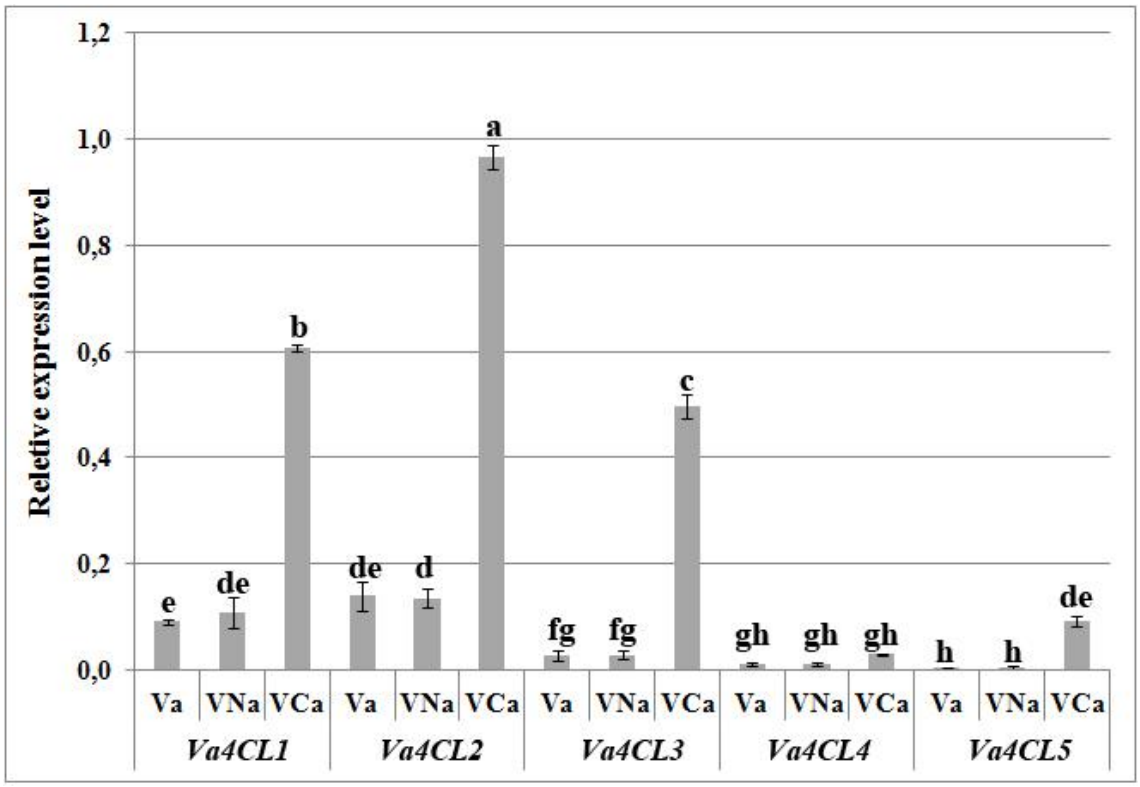

Fig. 7. Expression of *V. amurensis CDPK* genes in control callus culture (Va), callus line transformed with non-active *AtCPK1* (VNa) and callus line transformed with constitutively active *AtCPK1* (VCa). Data (mean ± standard error) represent measurements of three independent replicates from two different RNA isolations and are presented as relative expression levels normalized to the expression of the *V. vinifera* actin gene. Different letters above the bars indicate statistically significant differences of means ($P < 0.05$), Fisher's LSD.

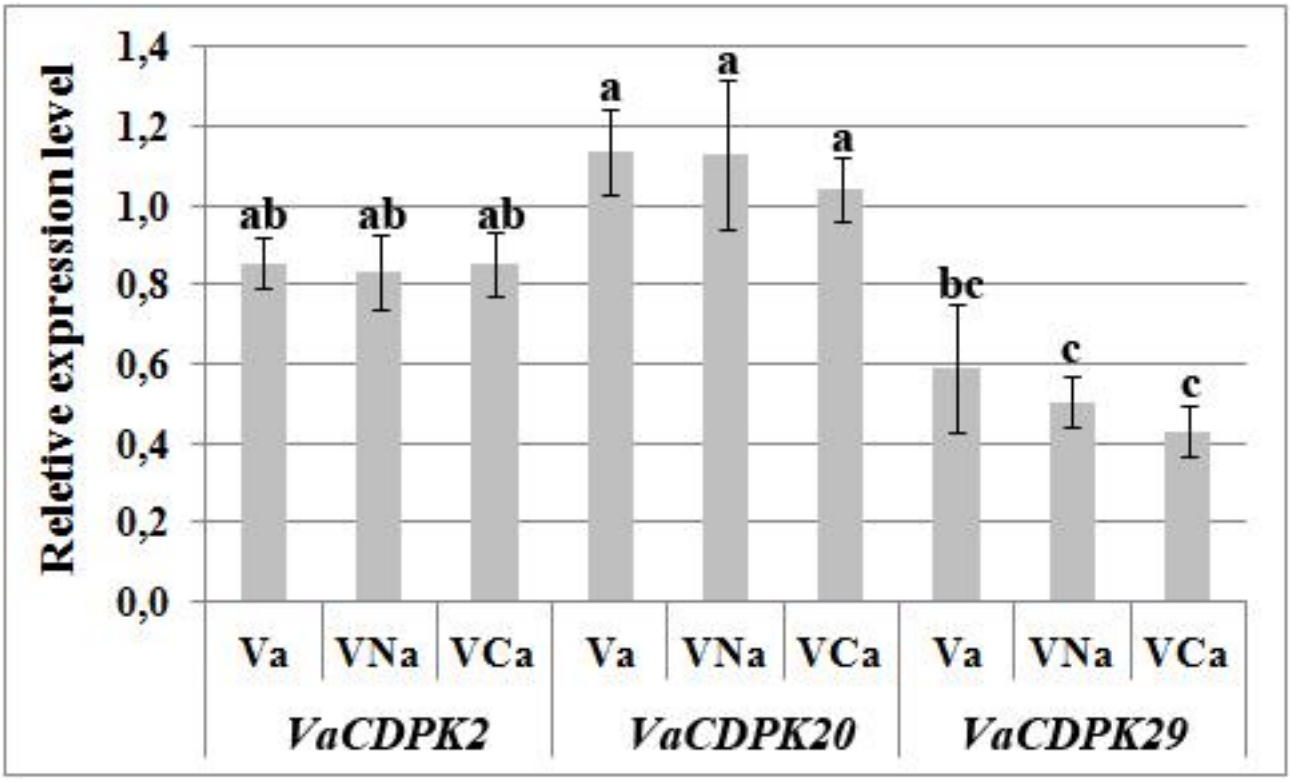

Fig. 8. CPK1-based sub-network of protein-protein interactions in *Arabidopsis*. GRF proteins are designated by the yellow-green color, CAMs by the light green color. The protein module SOS3-SOS2/CBL1-SIPK15-NDPK2 provides a link between CPK1, ROS signaling and cell stress resistance. The CPK1-GRF2-DHS1 pathway connects CPK1 with chorismate biosynthesis. The CPK1-ERS2 interactions links CPK1 with ethylene and cytokinin signaling (see also Bulgakov et al. 2016). CBL1, calcineurin B-like protein 1; CIPK15, CBL-interacting protein kinase 15; SOS2 (synonym: CIPK24, CBL-interacting protein kinase 24); SOS3 (synonym: CBL4, calcineurin B-like protein 4); SOS1, the plasma membrane Na^+/H^+ antiporter; CAMs, calmodulins; NDPK2, nucleoside diphosphate kinase 2; GF 14 PHI 14-3-3, 14-3-3 protein G-box factor14 PHI; GRF2, 14-3-3 protein G-box factor14 OMEGA; WIRKYs, WRKY transcription factors; BZR1, brassinazole-resistant 1 protein; ERS2, ethylene response sensor 2; CLV2, receptor protein kinase CLAVATA1.

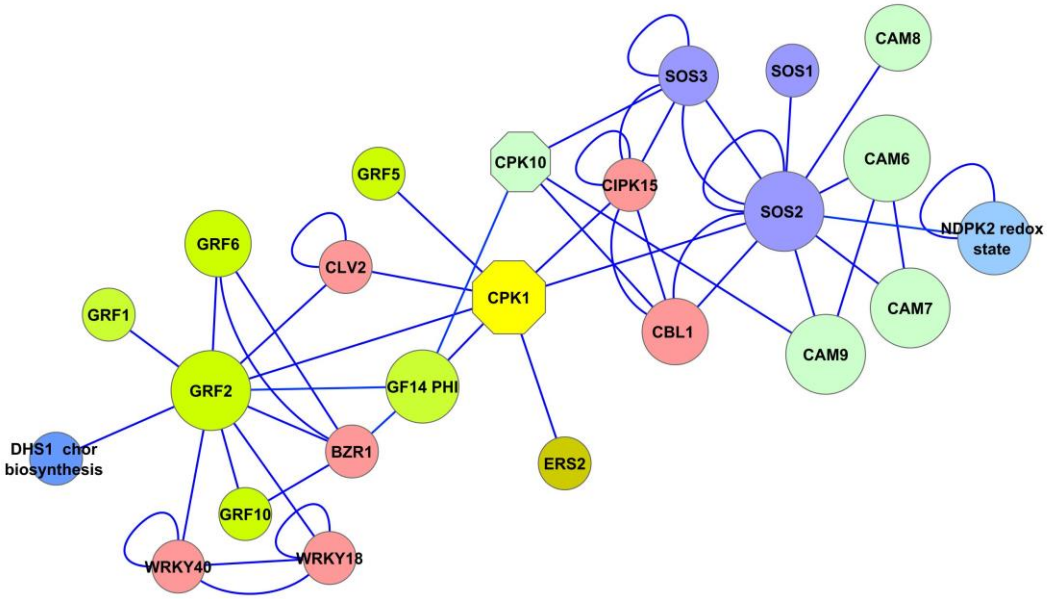

Table 1. The HPLC-ESI-HRMS analysis of stilbene derivatives from *Vitis amurensis* callus cultures

Peak no.*	Rt 1** (min)	Rt 2*** (min)	Negative ion mode			Positive ion mode			Elemental composition	Assignment
			$[M–H]^–$ (*m/z* detected)	$[M–H]^–$ (*m/z* calculated)	MS^2 (parent ion $[M–H]^–$) (*m/z*)	$[M+H]^+$ (*m/z* detected)	$[M+H]^+$ (*m/z* calculated)	MS^2 (parent ion $[M+H]^+$) (*m/z*)		
1	12.8	10.7	551.1771	551.1770	389.1236 (100) **** 227.0708 (44)	553.1918	553.1916	535.1817 (8) **** 517.1711 (8) 499.1603 (3) 391.1396 (100) 373.1288 (18) 355.1180 (15) 337.1076 (9) 295.0972 (11) 271.1336 (9) 253.1229 (11) 241.0865 (23) 229.0867 (54)	$C_{26}H_{32}O_{13}$	*trans*-resveratrol di-glucoside
2	15.5	13.6	389.1247	389.1242	227.0707 (100)	391.1393	391.1388	373.1286 (6) 355.1178 (13) 295.0970 (6) 271.1338 (5) 253.1231 (7) 241.0864 (4) 229.0863 (100) 135.0453 (3)	$C_{20}H_{22}O_8$	*trans*-piceid

3	18.5	16.6	227.0718	227.0714	185.0612 (100) 183.0818 (21) 159.0819 (23) 157.0661 (16) 143.0506 (53)	229.0864	229.0859	211.0760 (21) 193.0651 (4) 183.0811 (9) 165.0702 (2) 145.0651 (2) 135.0448 (100) 119.0495 (15) 107.0493 (27) 91.0546 (5)	$C_{14}H_{12}O_3$	*trans*-resveratrol
4	20.9	18.8	453.1346	453.1343	435.1242 (19) 411.1244 (10) 369.1134 (12) 359.0921 (100) 347.0919 (48) 333.0761 (12) 289.0863 (7) 253.0496 (14)	455.1496	455.1489	437.1378 (31) 361.1073 (75) 349.1075 (100) 343.0970 (55) 267.0662 (7) 255.0661 (42) 251.0711 (18) 239.0709 (26) 215.0711 (85) 199.0763 (42)	$C_{28}H_{22}O_6$	*trans*-ε-viniferin
5	22.0	19.9	453.1345	453.1343	435.1240 (79) 411.1241 (80) 369.1135 (100) 359.0928 (28) 347.0927 (24) 333.0769 (46) 317.0810 (11) 307.0970 (12)	455.1494	455.1489	437.1372 (58) 361.1069 (100) 343.0975 (11) 331.0970 (12) 313.0865 (17) 251.0713 (15) 237.0548 (26) 227.0708 (10)	$C_{28}H_{22}O_6$	*trans*-δ-viniferin

* Peaks are numbered as shown in Fig. 2, Fig. 3 and Fig. 4.

** The retention times of studied stilbenes were obtained by using LCMS-IT-TOF mass-spectrometer (Shimadzu, Japan)

*** The retention times of studied stilbenes were obtained by using an Agilent Technologies 1260 Infinity LC system (Agilent Technologies, USA)

**** Fragment ion intensity (% of the base peak) is shown in parentheses.

Table 2. Biomass accumulation and resveratrol production in the control and *AtCDPK*-transformed callus cultures of *V. amurensis*

Callus cultures	Fresh biomass (g L^{-1}) [a]	Dry biomass (g L^{-1}) [a]	Resveratrol content, % DW [b]	Resveratrol production (mg L^{-1})
Va	320±8[b]	10.5±1.1[b]	0.005±0.0006[b]	0.51±0.11[b]
V-Na	324±18[b]	11.2±1.5[b]	0.004±0.0011[b]	0.56±0.21[b]
V-Ca	576±10[a]	15.3±0.6[a]	0.424±0.0548[a]	69.7±8.72[a]

[a] Mean values ± SE are presented for growth parameters. The experiments were repeated four times (with ten replicates each) during long time (two-year) cultivation of the cultures.

[b] Data are presented as mean ± SE from four biological replicates (callus subcultures obtained with 3 month intervals) with two technical replicates for each biological replicate.

Different letters (superscript) indicate statistically significant differences of means ($P < 0.05$) in the rows, Fisher's LSD.

Table 3. Comparison of the deduced 4-coumarate-CoA ligase proteins from *V. amurensis* with corresponding enzymes from other plants

	A closest BLAST homolog among plant 4CLs, GenBank Accession no. (in parentheses), % identity at the protein level
Va4CL1	*Vitis vinifera* 4CL2 (XP_002272782), 99%; *Jatropha curcas* 4CL2 (XP_012074070), 83%; *Betula pendula* 4CL4 (AIR95613), 82%; *Ricinus communis* 4CL2 (XP_002533186), 81%
Va4CL2	*V. vinifera* 4CL7 (XP_002276353), 96%; *Ziziphus jujuba* 4CL7 (XP_015874554), 73%; *R. communis* 4CL7 (XP_002523698), 72%; *Morus alba* 4CL7 (AOV62758), 73%
Va4CL3	*V. vinifera* 4CL5 (XP_002285920), 91%; *Gossypium hirsutum* 4CL5 (XP_016741834), 75%; *Citrus sinensis* 4CL5 (XP_006473755), 75%; *Humulus lupulus* CCL5 (AGA17922), 74%
Va4CL4	*V. vinifera* 4CL9 (XP_010663724), 98%; *Jatropha curcas* 4CL9 (XP_012079878), 63%; *Populus euphratica* 4CL9 (XP_011044186), 65%; *Salix arbutifolia* Ca4CL5 (AGO89322), 64%
Va4CL5	*V. vinifera* 4CL2 (XP_002274994), 99%; *Betula platyphylla* 4CL1 (AKN79311), 84%; *R. communis* 4CL2 (XP_002520028), 83%; *Theobroma cacao* 4CL2 (XP_007029575), 82%